J|A|C|S
ARTICLES
Published on Web 03/14/2002

Reactions of *N*-Methyl-*N*-(4-biphenylyl)nitrenium Ion with Electron-Rich Arenes: Laser Flash Photolysis and Product Studies

Dominic Chiapperino, Sean McIlroy, and Daniel E. Falvey*

Contribution from the Department of Chemistry and Biochemistry, University of Maryland, College Park, Maryland 20742

Received April 25, 2001. Revised Manuscript Received October 11, 2001

Abstract: An arylnitrenium ion, *N*-methyl-*N*-(4-biphenylyl)nitrenium ion, was generated through photolysis of 1-(*N*-methyl-*N*-4-biphenylyl)amino-2,4,6-trimethylpyridinium tetrafluoroborate, and its reactions with various donor-substituted arenes (e.g., 1,3,5-trimethoxybenzene, mesitylene, 1,4-dimethoxybenzene, hexamethylbenzene, etc.) were examined using product analysis and laser flash photolysis. In general, trapping of the short-lived nitrenium ion by the arenes leads to three types of products: (1) the parent amine, *N*-methyl-*N*-4-biphenylylamine; (2) an ortho-adduct, where the ring position ortho to the nitrenium ion center is bonded to the arene ring; and (3) an N-adduct, where the nitrenium ion nitrogen is bonded to the trap. Laser flash photolysis studies show that the rates of these trapping reactions vary from 10^4 to 10^9 M^{-1} s^{-1}, depending on the structure of the arene trap. These trapping rate constants do not correlate with the one-electron oxidation potential of the arene, nor with the expected stability of a σ-complex derived from direct electrophilic aromatic substitution. It is argued that the observed rate constants correspond to initial formation of a π-complex between the arylnitrenium ion and the arene trap. This complex then forms the observed products.

Nitrenium ions are short-lived, electrophilic intermediates having the general structure $RR'N^+$.[1−4] Certain arylnitrenium ions (i.e., those where one of the ligands on nitrogen is an aromatic ring, e.g., **1** in Scheme 1) are intermediates in the mechanism of electrophilic DNA damage caused by metabolically activated arylamines or nitroarenes.[5−13] This proposal has inspired an intense interest in the lifetimes and decay pathways for various arylnitrenium ions. The most widely characterized decay pathway for arylnitrenium ions involves addition of nucleophiles (water, alcohols, halide ions, etc.) to the ring positions ortho and para to the nitrenium ion center.

Scheme 1

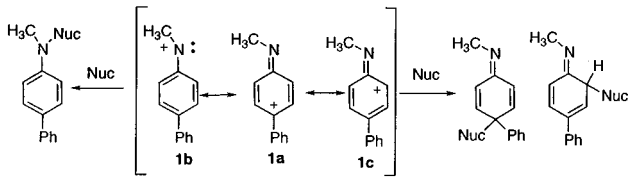

The propensity of the arylnitrenium ions to trap such nucleophiles on the ring is readily explained by the resonance hybrid **1a** which features delocalization of the positive charge onto the ring carbons. The importance of this structure has been verified by a number of ab initio MO calculations[14−19] and, more recently, by time-resolved IR spectroscopy. [20,21] A second, though less studied, decay route for singlet arylnitrenium ions is the addition of electron-rich alkenes and arenes to the nitrogen.[22−27] For example, Novak et al.[28,29] have documented

* To whom correspondence should be addressed. E-mail: df37@umail.umd.edu.

(1) Abramovitch, R. A.; Jeyaraman, R. In *Azides and Nitrenes: Reactivity and Utility*; Scriven, E. F. V., Ed.; Academic: Orlando, FL, 1984; pp 297−357.
(2) Simonova, T. P.; Nefedov, V. D.; Toropova, M. A.; Kirillov, N. F. *Russ. Chem. Rev.* **1992**, *61*, 584−599.
(3) McClelland, R. A.; Kahley, M. J.; Davidse, P. A. *J. Phys. Org. Chem.* **1996**, *9*, 355−360.
(4) Falvey, D. E. In *Organic, Physical, and Materials Photochemistry*; Ramamurthy, V., Schanze, K. S., Eds.; Marcel Dekker: New York, 2000; Vol. 6, pp 249−284.
(5) Miller, J. A. *Cancer Res.* **1970**, *30*, 559−576.
(6) Scribner, J. D.; Naimy, N. K. *Cancer Res.* **1975**, *35*, 1416−1421.
(7) Garner, R. C.; Martin, C. N.; Clayson, D. B. In *Chemical Carcinogens*, 2nd ed.; Searle, C. E., Ed.; American Chemical Society: Washington, DC, 1984; Vol. 1, pp 175−276.
(8) Kadlubar, F. F.; Beland, F. A. In *Polycyclic Hydrocarbons and Carcinogesis*; Harvey, R. G., Ed.; American Chemical Society: Washington, DC, 1985.
(9) Famulok, M.; Boche, G. *Angew. Chem., Int. Ed. Engl.* **1989**, *28*, 468−469.
(10) Turesky, R. J.; Lang, N. P.; Butler, M. A.; Teitel, C. H.; Kadlubar, F. F. *Carcinogenesis* **1991**, *12*, 1839−1845.
(11) Humphreys, W. G.; Kadlubar, F. F.; Guengerich, F. P. *Proc. Natl. Acad. Sci. U.S.A.* **1992**, *89*, 8278−8282.
(12) Kadlubar, F. F. In *DNA Adducts Identification and Biological Significance*; Hemmink, A. D. K., Shuker, D. E. G., Kadlubar, F. F., Segerbäck, D., Bartsch, H., Eds.; University Press: Oxford, U.K., 1994; pp 199−216.
(13) Novak, M.; Kennedy, S. A. *J. Phys. Org. Chem.* **1998**, *11*, 71−76.
(14) Li, Y.; Abramovitch, R. A.; Houk, K. N. *J. Org. Chem.* **1989**, *54*, 2911−2914.
(15) Ford, G. P.; Herman, P. S. *J. Mol. Stuct.* **1991**, *236*, 269−282.
(16) Falvey, D. E.; Cramer, C. J. *Tetrahedron Lett.* **1992**, *33*, 1705−1708.
(17) Cramer, C. J.; Dulles, F. J.; Falvey, D. E. *J. Am. Chem. Soc.* **1994**, *116*, 9787−9788.
(18) Sullivan, M. B.; Brown, K.; Cramer, C. J.; Truhlar, D. G. *J. Am. Chem. Soc.* **1998**, *120*, 11778−11783.
(19) Novak, M.; Lin, J. *J. Org. Chem.* **1999**, *64*, 6032−6040.
(20) Srivastava, S.; Toscano, J. P.; Moran, R. J.; Falvey, D. E. *J. Am. Chem. Soc.* **1997**, *119*, 11552−11553.
(21) Srivastava, S.; Ruane, P. H.; Toscano, J. P.; Sullivan, M. B.; Cramer, C. J.; Chiapperino, D.; Reed, E. C.; Falvey, D. E. *J. Am. Chem. Soc.* **2000**, *122*, 8271−8278.
(22) Takeuchi, H.; Hayakawa, S.; Murai, H. *J. Chem. Soc., Chem. Commun.* **1988**, 1287−1289.

addition of *N*,*N*-dimethylaniline to para-substituted phenyl nitrenium ions. Studies from this laboratory have characterized the addition of electron-rich alkenes to the nitrogen of the diphenylnitrenium ion.[30] The DNA base guanine also forms a similar adduct on the nitrogen (eq 1).[6,11,31−35] However, the mechanism of this addition remains controversial, and it is still unclear what factors dictate the regiochemical preferences. The conducting polymer, polyaniline (PANI), is formed through electrochemical and chemical oxidation of aniline. Several groups have argued that the key step involves coupling of the phenylnitrenium ion with aniline.[36−38] This mechanism, too, is controversial, and competitive trapping experiments have been interpreted as favoring an alternative radical cation mechanism, at least for the initial dimerization step.[39,40] In any case, both of these examples illustrate the need for clearer information regarding arylnitrenium ion/arene interactions. At present, there is little or no direct data regarding the rates of arylnitrenium ion addition to arenes, nor is it clear how the rates of these addition reactions are affected by substitutions on the arene.

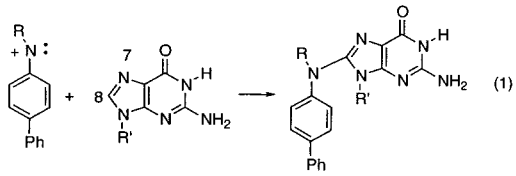

The following study was carried out with the goal of identifying various pathways by which arylnitrenium ions react with donor-substituted arenes. It was also of interest to determine how the rate of such reactions responds to changes in the structure of the arene. The particular nitrenium ion employed in these studies is *N*-methyl-*N*-(4-biphenylyl)nitrenium ion **1**. This species was chosen for study for several reasons. First, it has already been characterized by LFP and time-resolved IR experiments.[21] Second, the lifetimes and reaction rates of several related arylnitrenium ions with 4-phenyl substituents have been studied by LFP and competitive trapping experiments.[3,41−44] The presence of the 4-phenyl group substantially stabilizes the nitrenium ion relative to reactions with simple nucleophiles. Thus, it was anticipated that this nitrenium ion would exhibit a greater kinetic discrimination in its reaction with various arenes, allowing for a clearer picture of its selectivity. The stabilization afforded by the 4-phenyl substituent also gives the arylnitrenium ion a longer lifetime, allowing observation of its reactions with less reactive traps. Finally, the photochemical precursor to this nitrenium ion, **2** (eq 2), has a strong absorption band in the high wavelength UV region. This allows for LFP generation of the nitrenium ion using excitation wavelengths (355 nm) which are not absorbed by the simple arenes employed as traps.

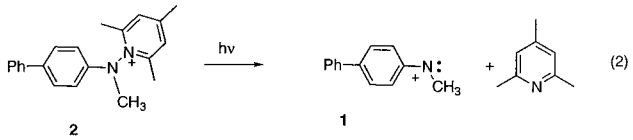

2 1

The following describes product studies and LFP experiments carried out on **1** with various donor-substituted arenes. LFP experiments show that the arenes react with **1** having rate constants (k_{trap}) that vary from 10^4 to 10^{10} M^{-1} s^{-1}. No intermediates are detected following the quenching process. The k_{trap} values do not correlate with either the oxidation potential of the arenes or their equilibrium constant for protonation by strong acid. There is, however, a good correlation with the ability of the same arenes to form π-complexes with electron-poor arenes. It is argued that the rate-determining step involves initial π-complexation followed by formation of a longer-lived σ-complex. The latter is the precursor to the observed stable products.

Results

Structures of the Stable Products. Synthesis and characterization of the nitrenium ion's precursor **2** are described elsewhere.[21] As has been demonstrated earlier, photolysis of this compound produces both nitrenium ion **1** and 2,4,6-trimethylpyridine through a N−N bond heterolysis (eq 2). The latter is stable and is normally recovered in nearly quantitative yields from the photolysis mixtures. When nitrenium ion **1** is generated in the presence of various donor-substituted arenes (Chart 1), stable products resulting from addition of the arene to both the ortho-phenyl ring position and the nitrogen are formed. The parent amine **3** is also observed, which formally can be considered to result from addition of two electrons and one proton to the nitrenium ion **1**. Scheme 2 depicts the general result.

Chart 2 and Table 1 report specific results from trapping with each individual arene. A common procedure for the preparative photolyses was used in all cases unless otherwise noted. The solutions for photolysis were purged with nitrogen before and during photolysis and irradiated only at wavelengths >320 nm to ensure that none of the arenes absorb light. Photoprecursor **2**, arene quencher, and small amounts of perchloric acid (9 mM) were present in these MeCN solutions. The purpose of the latter is to protonate the amine products so that they will not be consumed by secondary oxidation reactions. The temperature of solutions throughout the photolysis was maintained at 22 (±3) °C using a water-jacketed quartz cell. In most cases, the adducts

(23) Novak, M.; Martin, K. A.; Heinrich, J. L. *J. Org. Chem.* **1989**, *54*, 5430−5431.
(24) Helmick, J. S.; Martin, K. A.; Heinrich, J. L.; Novak, M. *J. Am. Chem. Soc.* **1991**, *113*, 3459−3466.
(25) Helmick, J. S.; Novak, M. *J. Org. Chem.* **1991**, *56*, 2925−2927.
(26) Takeuchi, H.; Adachi, T.; Nishiguchi, H.; Itou, K.; Koyama, K. *J. Chem. Soc., Perkin Trans. 1* **1993**, 867−880.
(27) Takeuchi, H.; Watanabe, K. *J. Phys. Org. Chem.* **1998**, *11*, 478−484.
(28) Novak, M.; Rangappa, K. S. *J. Org. Chem.* **1992**, *57*, 1285−1290.
(29) Novak, M.; Rangappa, K. S.; Manitsas, R. K. *J. Org. Chem.* **1993**, *58*, 7813−7821.
(30) Moran, R. J.; Cramer, C. J.; Falvey, D. E. *J. Org. Chem.* **1996**, *61*, 3195−3199.
(31) Famulok, M.; Bosold, F.; Boche, G. *Angew. Chem., Int. Ed. Engl.* **1989**, *28*, 337−338.
(32) Bosold, F.; Boche, G. *Angew. Chem., Int. Ed. Engl.* **1990**, *29*, 63−64.
(33) Novak, M.; Kennedy, S. A. *J. Am. Chem. Soc.* **1995**, *117*, 574−575.
(34) Gu, Z.; Gorin, A.; Hingerty, B. E.; Broyde, S.; Patel, D. *Biochemistry* **1999**, *38*, 10855−10870.
(35) McClelland, R. A.; Ahmad, A.; Dicks, A. P.; Licence, V. *J. Am. Chem. Soc.* **1999**, *121*, 3303−3310.
(36) Genies, E. M.; Lapowski, M. *J. Electroanal. Chem.* **1987**, *236*, 189−197.
(37) Wei, Y.; Tang, X.; Sun, Y. *J. Polym. Sci., Part A: Polym. Chem.* **1989**, *27*, 2385−2396.
(38) Wei, Y.; Jang, G.-W.; Chan, C. C.; Hsueh, K. F.; Hariharan, R.; Patel, S.; Whitecar, C. K. *J. Phys. Chem.* **1990**, *94*, 7716−7721.
(39) Lux, F. *Polym. Rev.* **1995**, *35*, 2915.
(40) Ding, Y.; Padias, A. B.; Hall, J. H. K. *J. Polym. Sci., Part A: Polym. Chem.* **1999**, *37*, 2569−2579.
(41) Novak, M.; Kahley, M. J.; Eiger, E.; Helmick, J. S.; Peters, H. E. *J. Am. Chem. Soc.* **1993**, *115*, 9453−9460.
(42) Davidse, P. A.; Kahley, M. J.; McClelland, R. A.; Novak, M. *J. Am. Chem. Soc.* **1994**, *116*, 4513−4514.
(43) Robbins, R. J.; Laman, D. M.; Falvey, D. E. *J. Am. Chem. Soc.* **1996**, *118*, 8127−8135.
(44) Ren, D.; McClelland, R. A. *Can. J. Chem.* **1998**, *76*, 78−84.

Chart 1

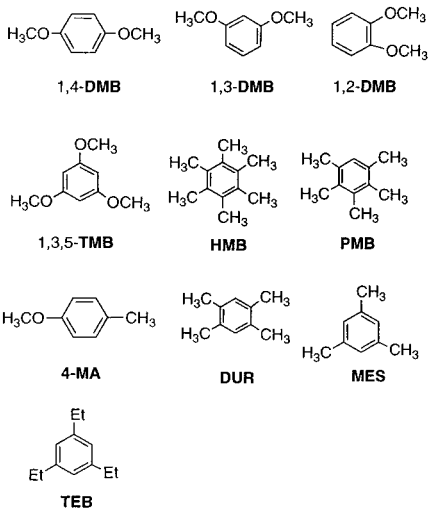

Scheme 2

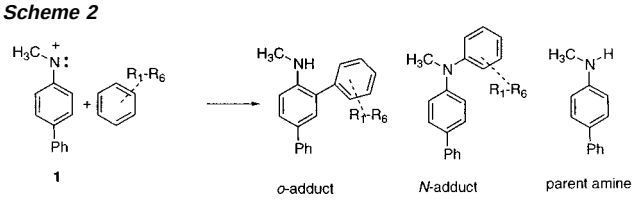

Chart 2

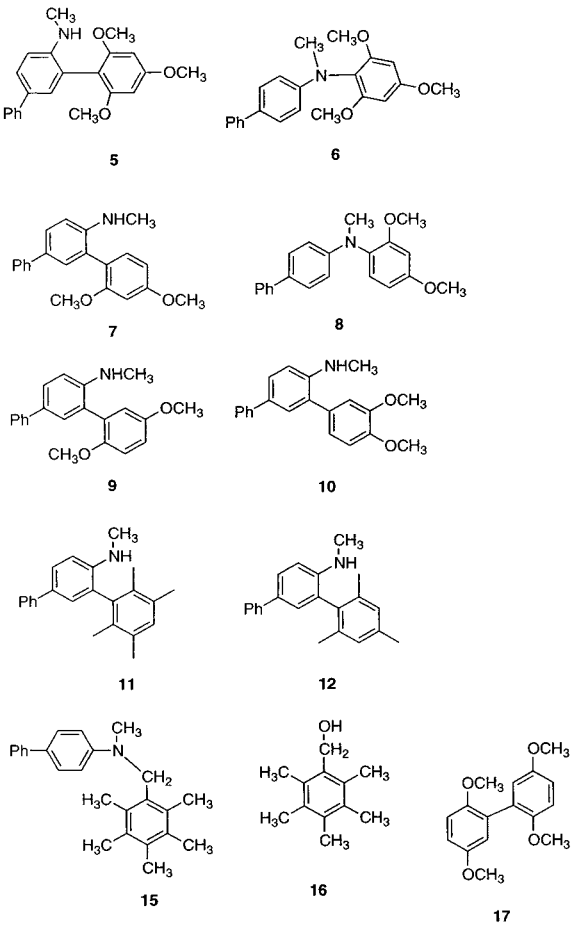

were generated from preparative photolysis, isolated, and characterized as pure materials. In some cases, low yields and/or complex reaction mixtures precluded the isolation of certain products in sufficient quantities to allow for complete characterization. Where noted, the structures are inferred from GC/MS fragmentation patterns. In other cases, the yields of the products were ascertained from integration of their peaks in the ^{1}H NMR spectrum of the crude photolysis mixture.

Table 1. Product Distributions from Photolysis of **2** in the Presence of Various Arenes

arene[a]	product structure[a]	% yield	method of yield measurement
TMB	**3**	43	isolated
	5	27	isolated
	6	11	isolated
1,3-DMB	**3**	49	isolated
	7	21	isolated
	8	11	isolated
HMB	**3**	72	^{1}H NMR
1,4-DMB	**3**	27	isolated
	9	67	isolated
1,2-DMB	**3**	74	^{1}H NMR
	10	trace	GC/MS
DUR	**3**	46	^{1}H NMR
	11	trace	GC/MS
MES	**3**	44	isolated
	12	52	isolated
1,4-DMB/MES[b]	**3**	38	GC
	9	37	GC
	12	0.83	GC

[a] Structure abbreviations are defined in Chart 1. [b] 1:5.4 ratio of 1,4-DMB to MES.

Trapping of **1** by TMB produces parent amine **3** as the major product along with ortho-addition product **5** and N-addition product **6** in an approximately 2:1 ratio. 1,3-DMB gives an analogous result. Again **3** is the major product, and it is accompanied by formation of the ortho- and N-adducts (**7** and **8**, respectively) in an ca. 2:1 ratio. With 1,4-DMB, the major product is the ortho-adduct **9** with parent amine **3** formed in much lower yield. No N-adduct was detected with this trap, but compound **17**, derived from oxidative dimerization of 1,4-DMB, was detected in minor (<5%) amounts. Mesitylene (MES) behaves in a similar way: the ortho-adduct (**12**) yield exceeds the yield of the parent amine (**3**), although the ratio is smaller than that with 1,4-DMB.

In contrast, DUR and 1,2-DMB trap the nitrenium ion to give parent amine **3** with only trace amounts of ortho addition products (**11** for DUR and **10** for 1,2-DMB) observed with these two traps. Hexamethylbenzene (HMB) gives high yields of **3** along with two interesting minor products: one (**15**) derived from a formal insertion of the nitrenium center into the CH bond of the trap, and the other (**16**) derived from a net oxygen insertion into the C−H bond of the trap.

To assess the relative reactivity of the arene traps, a competition experiment was carried out. Nitrenium ion **1** was generated in the presence of both MES (144 mM) and 1,4-DMB (26.5 mM), and the product mixture was analyzed by GC. As expected, we get adducts of both traps, along with the parent amine **3**. Assuming irreversible formation of the π-complex, the ratio of addition rate constants, k_{DMB}/k_{MES}, can be predicted using eq 3.

$$\frac{k_{DMB}^{predicted}}{k_{MES}^{predicted}} = \frac{1.4Y_9}{1.9Y_{12}} \times \frac{[MES]}{[DMB]} \qquad (3)$$

where Y_9 and Y_{12}, are the yields of products **9** and **12**,

Scheme 3

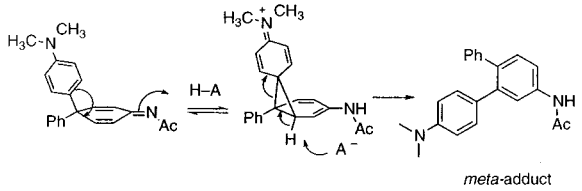

Table 2. ^{1}H NMR Data for Isolated Ring Adducts

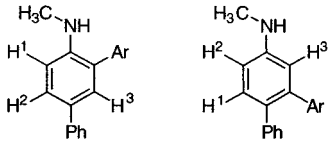

ring adducts (arene)	H-1 ppm (coupling constants)	H-2 ppm	H-3 ppm
5 (TMB)	6.78 (8.4 Hz)	7.53 (8.4, 2.3 Hz)	7.29 (2.3 Hz)
8 (1,3-DMB)	6.83 (8.4 Hz)	7.52 (8.4, 2.3 Hz)	7.33 (2.3 Hz)
9 (1,4-DMB)	6.65 (8.4 Hz)	7.51 (8.4, 2.3 Hz)	7.27 (2.3 Hz)
12 (MES)	6.75 (8.4 Hz)	7.54 (obscured)	7.21 (2.3 Hz)
ortho adduct[a]	6.86 (8.0 Hz)	7.51 (8.0, 2.5 Hz)	7.78 (2.5 Hz)
meta adduct[a]	7.61 (8.0 Hz)	6.76 (8.0, 2.5 Hz)	7.03 (2.5 Hz)

[a] Predicted chemical shifts and coupling constants from literature assuming Ar═Ph.

respectively and the ratio 1.4/1.9 accounts for the formation of the common product, **3**, from both trapping pathways. The results of this experiment provide a value of 183, demonstrating that 1,4-DMB is more reactive than MES.

One of the issues confronted in these product studies was the assignment of the substitution pattern in the ring adducts. The 1,3,4-trisubstituted biphenyl derivative (ortho-adduct) is the assigned structure in all of the specific cases described below. Theoretically, a 1,2,4-derivative, or "meta-adduct", is plausible as well and would be consistent with the arene adducts isolated from DMA trapping in Novak's work. In that study, the meta-adducts were the major product isolated, with much smaller yields of ortho- and N-adducts. The meta-adducts are believed to form as the result of 1,2-aryl group migration from a para-substituted cyclohexadienyl imine (Scheme 3).

The structural assignment of the products from this study as ortho-adducts is based on comparison of chemical shifts for aromatic signals in the ^{1}H NMR spectra with those derived from model calculations. Both the meta- and the ortho-adducts are predicted to show three types of aromatic proton resonances: a strongly (ortho) coupled doublet, defined as H-1, a double-doublet, defined as H-2, and a weakly (meta) coupled doublet, defined as H-3. Both of these structures are shown in Table 2. The predicted chemical shifts are calculated using eq 4 in which the effects of the various ring substituent on the chemical shift δ_H are given by an empirically derived parameter (Z) and its position on the benzene ring (i) relative to the observed proton. Because of limited literature data, the arene residue was treated as a simple phenyl ring. The model coupling constants were assumed as 8.0 for ortho coupling and 2.5 for meta coupling.

$$\delta_{Hi} = 7.26 + \sum_i Z_i \qquad (4)$$

Because of its significant shielding effect on ortho protons, the methylamino substituent is expected to place the strongly coupled doublet (H-1) in the ortho-adduct the furthest upfield. In contrast, the model spectrum of the meta-adduct predicts the doublet of doublets (H-2) to be the furthest upfield, and the strongly coupled doublet, H-1, should be furthest downfield. As is apparent from the experimental data in Table 2, the isolated ring adducts are more consistent with the pattern predicted for the ortho adduct. Both H-1 and H-2 show excellent quantitative agreement with the predicted values. In the case of H-3, the quantitative agreement is less satisfactory, the experimental chemical shifts being consistently 0.5 ppm lower than the model value. This can be attributed to the fact that the model calculations assume the arene residue to be benzene, rather than a donor-substituted aromatic ring. The H-3 proton, being nearest to the arene substituent in both structures, would be expected to show the largest deviation from the predicted value.

Scheme 4. Electron Transfer/Radical Combination Mechanism

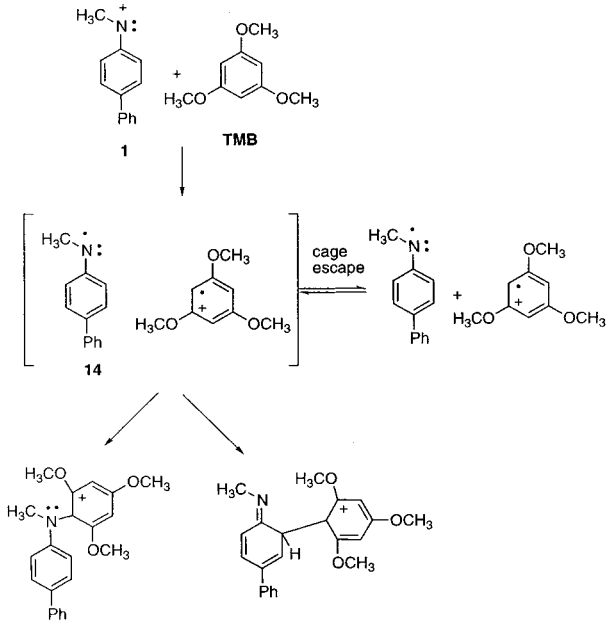

Laser Flash Photolysis Studies: A Search for Intermediates. One of the proposed mechanisms by which nitrenium ions could add to arenes is through an initial one-electron-transfer reaction followed by either in-cage (geminate) or diffusive radical−radical cation coupling. This is illustrated for the case of TMB in Scheme 4. To the extent that the radical intermediates escape the geminate solvent cage, it should be possible to detect them by LFP. Previous studies have shown that the 4-biphenylylaminyl radical cation has broad absorption near 646 nm.[45] The radical cation arising from the putative electron-transfer pathway in our study, **22**, differs only in having an additional methyl group on the nitrogen. The latter is not expected to have a strong effect on the absorption maximum. To determine if the nitrenium ion-based radical intermediates could be detected, we generated these species by an alternative photochemical pathway. Lustzyk et al.[46,47] have shown that aminyl radicals can be generated through the photolysis of the corresponding *N*-nitrosamine derivatives. These radicals are reasonably basic; *N*-methylanilinyl radical (Ph(CH3)N•), for example, has a pK_a

(45) Shida, T. *Electronic Absorption Spectra of Radical Ions*; Elsevier: Amsterdam, 1988; p 446.
(46) Jonsson, M.; Wayner, D. D. M.; Lusztyk, J. *J. Phys. Chem.* **1996**, *100*, 17539−17543.
(47) Wagner, B. D.; Ruel, G.; Lusztyk, J. *J. Am. Chem. Soc.* **1996**, *118*, 13−19.

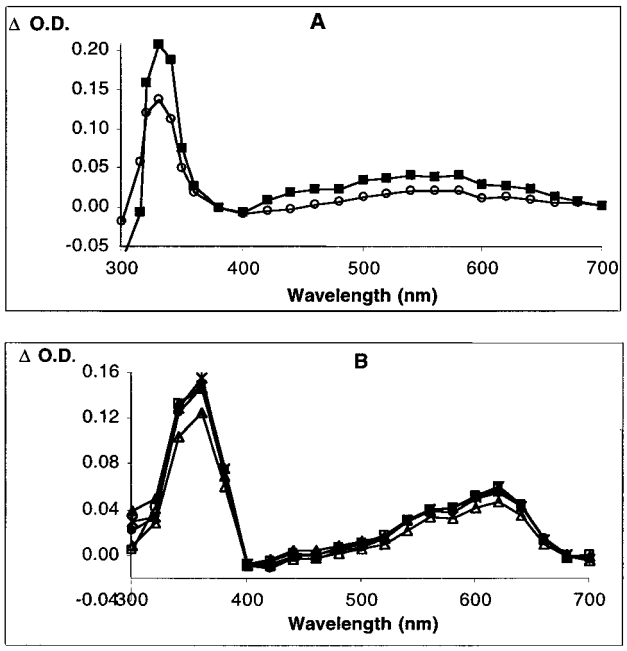

Figure 1. Transient spectra from LFP (308 nm, 10 ns, 25−50 mJ/pulse) of Nitrosoamine **20** at pH 8.5 (A**)** and pH 7.0 (B) aqueous solutions containg 10% CH_3CN.

Scheme 5. Independent Generation of Radical **21** and Radical Cation **22**

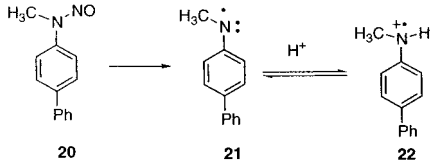

of 7.5. Thus, under protic conditions aminyl radicals are rapidly converted into their cation radical conjugate acids. This is illustrated in Scheme 5.

Using Lusztyk's method, both the neutral aminyl radical **22** and its conjugate acid (amine cation radical, **21**) were generated. Specifically, LFP of *N*-nitroso-*N*-methyl-*N*-(4-biphenylyl)amine **20** under protic conditions (pH 7.5) generates the transient spectrum in Figure 1B, which exhibits a maximum at 630 nm. We assign this species to the *N*-methyl-*N*-biphenylyl radical cation **21** on the basis of its similarity to the spectrum of its unmethylated radical. When the experiment is repeated under more basic conditions (pH 8.5), LFP generates the spectrum shown in Figure 1A, where the high wavelength peak is broader and shows a maximum at 560 nm. When **20** is photolyzed in CH_3CN containing trace amounts of water, the 560 nm peak is detected immediately following the excitation pulse, and it is converted into the 630 nm band showing clean isosbestic behavior (data not shown). We assume that this is due to protonation of the radical by adventitious water. We therefore assign the 560 nm band to the aminyl radical **22**.

The spectra of the cation radicals for many of the arene traps have also been characterized either by LFP or by low-temperature methods.[45] For example, the cation radical of HMB absorbs at 498 nm, the cation radical for 1,3-DMB has absorption maxima at 477 and 505 nm, the cation radical of TMB absorbs at 613 and 645 nm, and the cation radical of 1,4-DMB absorbs at 443 and 475 nm. Thus, the intermediates expected to arise from the proposed electron-transfer pathway

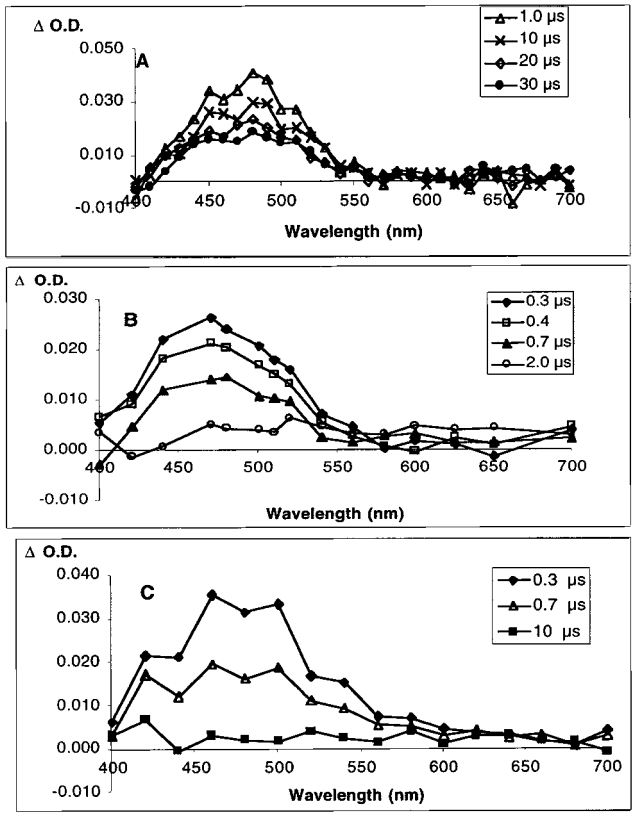

Figure 2. Transient spectra from LFP (355 nm, 6 ns, 1−2 mJ/pulse) of **2** in CH_3CN (generating nitrenium ion **1**) in the presence and absence of trapping agents: (A) no trap; (B) 29 mM TMB; (C) 57 mM HMB.

all absorb in the visible region of the spectrum, and they should be detectable by our technique.

No additional intermediates were detected when the nitrenium ion was generated in the presence of the various arenes. LFP experiments were carried out where a sufficient concentration of arene trap was added so that the lifetime of the nitrenium ion was diminished by 80%. The transient spectrum was then examined to determine if the radical intermediates resulting from the electron transfer were formed. Figure 2 shows several typical cases where nitrenium ion **1** was generated in the presence of 29 mM TMB, 57 mM HMB, and in the absence of any trapping agent. In each case, the only effect of the arene is to reduce the lifetime of the nitrenium ion. No new visible absorption bands appeared following the decay of the nitrenium ion signal. The starting material, **2**, absorbs in the region 300−400 nm, and any new intermediate species that absorbs in this region may be obscured by the loss of starting material. Elsewhere we will describe similar LFP studies of *N*,*N*-diphenylnitrenium ion with 1,4-DMB and several other electron-rich arenes. In that case, the radical intermediates are detected in a similar LFP experiment.

There are two situations where the radical intermediates could form but escape LFP detection: (1) if the radicals couple rapidly following their formation from electron transfer such that only a small, undetectable, fraction exits the geminate solvent cage (such cage lifetimes are typically regarded to be less than 1−2 ns), and (2) if the radicals form slowly, perhaps from an unstable adduct, they might exist in a very low steady-state concentration and elude detection. The latter case would rule out the possibility of a direct, one-step electron transfer, but would be consistent with radical formation by an addition/bond scission pathway.

Table 3. Reaction Rate Constants (k_{trap}, M^{-1} s^{-1}) for the Trapping of Nitrenium Ion **1** by Various Aromatic Compounds

trap	K_{trap}	E_{ox}	trap	K_{trap}	E_{ox}
DMA	1.3×10^{10}	0.53	PMB	$(2.5 \pm 0.3) \times 10^6$	1.71
TMB	$(1.7 \pm 0.5) \times 10^9$	1.49	4-MA	$(4.0 \pm 0.2) \times 10^5$	1.64
1,3-DMB	$(3.2 \pm 0.5) \times 10^8$	1.49	DUR	$(3.2 \pm 0.8) \times 10^5$	1.78
HMB	$(1.2 \pm 0.6) \times 10^7$	1.59	MES	$(9.2 \pm 0.4) \times 10^4$	2.11
1,4-DMB	$(8.9 \pm 0.6) \times 10^6$	1.34	TEB	$(1.4 \pm 0.2) \times 10^4$	2.00
1,4-DMB-d_6	$(9.7 \pm 0.5) \times 10^6$		TOL	$(<4.0 \pm 1.0) \times 10^3$	2.40
1,2-DMB	$(6.5 \pm 0.5) \times 10^6$	1.45			

LFP Studies: Rate Constants for Trapping Reactions. The rate constants for the reactions of nitrenium ion **1** with various arenes (k_{trap}) were determined using LFP with the goal of learning how changes in trap structure affect the reactivity. As demonstrated earlier, LFP of precursor **2** generates nitrenium ion **1**, which can be detected at its λ_{max} of 480 nm. The pseudo-first-order decay constant (k_{obs}) of the arylnitrenium was determined at various concentrations of arene trap. Unless otherwise noted, all of these rate constants conformed well to the pseudo-first-order relationship (eq 5), where k_o is the decay rate constant in the absence of trapping agent, k_{trap} is the second-order rate constant for the reaction of the nitrenium ion with the arene, and [*T*] is the concentration of the arene trap. The k_{trap} values for various arenes are compiled in Table 3, along with the electrochemical oxidation potentials (E_{ox}) for each arene taken from previous studies.[48,49]

$$k_{obs} = k_o + k_{trap}[T] \quad (5)$$

In most cases, the kinetic experiments were carried out by adding small amounts of the trap to solutions of the photoprecursor **2** and by measuring the decay kinetics of **1** which were generated by LFP. In the case of HMB, low solubility prevented measurement in neat CH_3CN, so the k_{trap} reported was determined in a 3:2 toluene−CH_3CN solvent mixture. The k_{trap} for toluene was estimated from comparison of the decay rate in neat CH_3CN to that in neat $PhCH_3$ and considering the molar concentration of pure toluene (8.4 M). Given the small change in k_{obs} and the fact that only two concentration points are used in the determination, this particular value should be regarded as an approximate upper limit.

The arenes react with the nitrenium ion **1** showing a wide range of rate constants. The k_{trap} values vary from 1.7×10^9 M^{-1} s^{-1} for TMB to 9.2×10^4 M^{-1} s^{-1} for MES. Even a casual inspection of Table 2 demonstrates that there is no correlation of k_{trap} with E_{ox}. For example, the readily oxidized substrate, 1,4-DMB ($E_{ox} = 1.34$ V), traps the nitrenium ion ca. 10^2 times more slowly than does TMB ($E_{ox} = 1.49$ V). Likewise, 1,2-DMB traps the nitrenium ion ca. 50 times more slowly than 1,3-DMB, even though both traps have approximately the same E_{ox}. Nor is k_{trap} determined solely by the nature of the substituent. For example, the alkyl derivatives and HMB and PMB are more reactive than the alkoxy derivative 4-MA. Finally, there is no simple correlation between the steric demands of the arene and the rate of trapping. Thus, HMB is more reactive than MES. Likewise, TMB is more reactive than 1,3-DMB. On the other hand, triethylbenzene (TEB) is slightly less reactive than MES, suggesting that if the electron-donating ability of the substituents is approximately equal, then steric effects might determine the rate of addition. Finally, we note that addition of the arenes increases the rate of nitrenium ion decay, but has no noticeable effect on the initial intensity of the nitrenium ion's absorbance. Thus, the traps react with nitrenium ion **1**, but there is no evidence that they react with a precursor to the nitrenium ion (e.g., the excited state of **2**).

Table 4. Reaction Rate Constants (k_{trap} M^{-1} s^{-1}) for the Trapping of Nitrenium Ion **1** by Various Oxygen-Based Nucleophiles

nucleophiles	k_{trap} (M^{-1} s^{-1})	nucleophiles	k_{trap} (M^{-1} s^{-1})
water	9.3×10^4	*n*-butyl alcohol	3.9×10^5
methanol	3.7×10^5	*sec*-butyl alcohol	2.5×10^5
ethanol	3.3×10^5	*tert*-butyl alcohol	1.8×10^5
n-propyl alcohol	3.0×10^5	tetrahydrofuran	5×10^4
isopropyl alcohol	1.9×10^5		

To probe for kinetic isotope effects, 1,4-DMB-d_6 was prepared wherein the methoxy groups were labeled with deuteriums. The k_{trap} was measured and compared with that for the unlabeled material. The 1,4-DMB-d_6 trap shows a slightly higher rate constant than DMB-h_6, although the difference is probably not statistically significant. In any case, it is clear that there is no primary kinetic isotope effect on the rate of the trapping reaction.

For comparison purposes, k_{trap} values for some oxygen-based nucleophiles were also characterized. These nucleophiles, listed with their rate constants in Table 4, include several simple alcohols (CH_3OH, ^iPrOH, etc.) and an ether, (tetrahydrofuran). In the case of the alcohols, the addition mechanism has been well established by previous work to involve complexation of the oxygen atom to the ring carbons of the arylnitrenium ion.[19,50−53] In the present study, the alcohols all trap the nitrenium ion with k_{nuc} values that fall in the remarkably narrow range of 1.8 to 3.9×10^5 M^{-1} s^{-1}, suggesting that k_{trap} is not particularly sensitive to the steric bulk of the nucleophile.

Discussion

Historically, the addition of electrophiles to arenes has been studied with respect to two general pathways. One involves initial formation of a π-complex, which involves a delocalized interaction of the electrophile with the arene, and the other involves a σ-complex, where the electrophile interacts specifically with one carbon atom. [54,55] These two intermediates are illustrated in Scheme 6. With simple electrophiles such as NO_2^+, Br_2, etc., the initial step is widely regarded to be formation of the σ-complex. The arylnitrenium ions are larger and have much more delocalized positive charge than do the simple electrophiles that have been classically associated with electrophilic aromatic substitution. Therefore, there was reason to suspect that its mode of addition may be different than these more localized electrophiles.

The rates for nitrenium ion arene reaction correlate with the equilibrium constant for π-complexation. Figure 3 compares log-

(48) Eberson, L. *Electron-Transfer Reaction in Organic Chemistry*; New York, Springer-Verlag 1987.
(49) Rathore, R.; Kochi, J. K. *Adv. Phys. Org. Chem.* **2000**, *35*, 193−317.
(50) Novak, M.; Kahley, M. J.; Lin, J.; Kennedy, S. A.; Swanegan, L. A. *J. Am. Chem. Soc.* **1994**, *116*, 11626−11627.
(51) Robbins, R. J.; Yang, L. L.-N.; Anderson, G. B.; Falvey, D. E. *J. Am. Chem. Soc.* **1995**, *117*, 6544−6552.
(52) Sukhai, P.; McClelland, R. A. *J. Chem. Soc., Perkin Trans. 2* **1996**, 1529−1530.
(53) Ramlall, P.; McClelland, R. A. *J. Chem. Soc., Perkin Trans. 2* **1999**, 225−232.
(54) Lowry, T. H.; Richardson, K. S. *Mechanism and Theory in Organic Chemistry*; Harper and Row: New York, 1987.
(55) Hubig, S. M.; Kochi, J. K. *J. Org. Chem.* **2000**, *65*, 6807−6818.

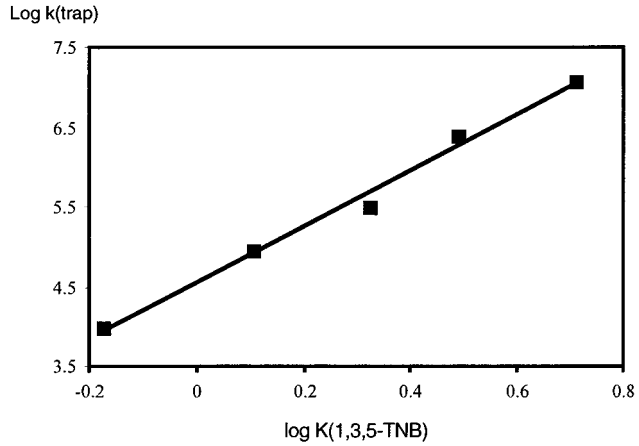

Figure 3. Relationship of trapping rate constants to the binding equilibrium constants for trinitrobenzene.

Scheme 6

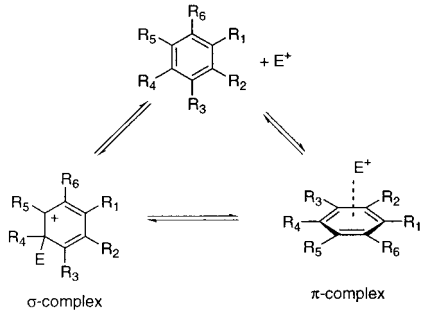

(k_{trap}) with log(K_{TNB}), where K_{TNB} is the equilibrium constant for the same arenes forming charge-transfer complexes with the trinitrobenzene (eq 6).[56] The alkyl-substituted benzenes all show an excellent linear free energy relationship when analyzed in this manner. This was compared with a similar plot of log(k_{trap}) and log(K_{HF}), where K_{HF} is the equilibrium constant for ring-protonation by a strong acid (HF, eq 7).[57] In this case, there is a much poorer correlation.

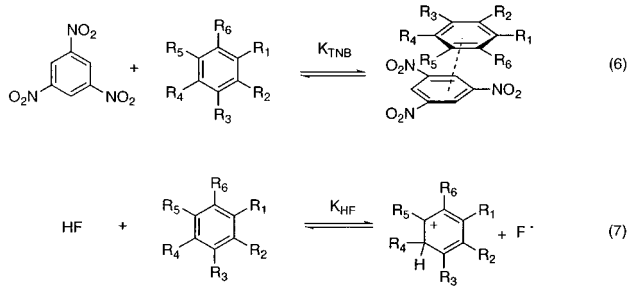

This linear free energy correlation favors a mechanism involving initial formation of a π-complex. However, only the alkylbenzenes were used for the comparison due to limited equilibrium data available in the literature. The possibility remains that the alkoxy derivatives react through an alternative mechanism. One alternative is the oxygen complexation pathway, shown in Scheme 7, in which the nonbonding electron pair on oxygen adds to one of the ring carbons of the nitrenium ion's phenyl ring. Indeed, simple alcohols add by this mechanism.[19,51,58] The k_{trap} for methanol should represent a conservative upper limit for the rate of oxygen complexation by the alkoxybenzenes. This is because the alkoxybenzenes are more sterically encumbered than methanol and because aromatic rings withdraw electron density from oxygen substituents, rendering them far less nucleophilic than simple alcohols or alkyl ethers. An earlier study[21] provides a k_{trap} value for methanol of 3.8×10^5 M^{-1} s^{-1}, which is slower than k_{trap} for any of the alkoxybenzene derivatives studied here. Furthermore, oxygen complexation would not be consistent with the observed effects of substitution on the rates. For example, 1,3-DMB has its two alkoxy groups in a meta arrangement. In this orientation, they ought to diminish each other's nucleophilicity. However, 1,3-DMB reacts more rapidly than does its 1,4-isomer in which the para-disposition of the alkoxy groups would be expected to reinforce each other's nucleophilicity through resonance. Thus, the oxygen complexation pathway is expected to contribute negligibly, if at all, to the observed k_{trap} values.

Scheme 7. Oxygen Complexation Mechanism

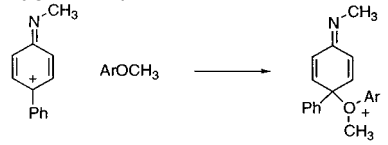

Scheme 8. Hydride and H Atom Transfer

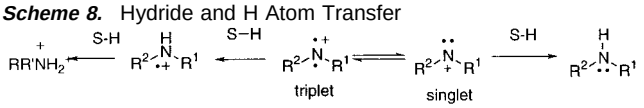

In many cases, σ-complexes of electrophiles with benzene derivatives are stable and can be characterized by UV−vis spectroscopy. For example, the σ-complex of nitronium ion (NO_2^+) with HMB has a λ_{max} at 430 nm with a molar absorptivity of nearly 10^4 M^{-1} cm^{-1}.[55] This suggests that any σ-complexes formed directly from the reaction of the arenes with the nitrenium ion ought to be detectable in the LFP experiments. The fact that no new signals are detected in the visible region following the decay of nitrenium ion can be taken as evidence, albeit of a negative kind, that σ-complexes are not formed immediately upon quenching of the nitrenium ion. The absorption maxima of the proposed π-complexes could, in principle, be predicted from the ionization potential of the arenes and the electron affinity of the nitrenium ion.[56] Unfortunately, the latter parameter is not known. It is possible that these complexes absorb with insufficient intensity and/or at wavelengths too low (<390 nm) to be detected under our conditions.

With all of the arenes, significant yields of the parent amine **3** are observed. This sort of product has been shown to arise from sequential H atom abstraction reactions of triplet state nitrenium ions,[59,60] and hydride transfer to singlet state nitrenium ions.[61] For example, the parent nitrenium ion, NH_2^+, has been shown to exhibit both of these behaviors (Scheme 8).[62] Nitrenium ion **1** has a singlet ground state with a singlet−triplet energy gap of −18.2 kcal/mol. This has been determined from

(56) Foster, R. *Organic Charge-Transfer Complexes*; Academic: New York, 1969.
(57) Andrews, L. J.; Keefer, R. M. *Molecular Complexes in Organic Chemistry*; Holden-Day: San Francisco, 1964.
(58) Novak, M.; Kahley, M. J.; Lin, J.; Kennedy, S. A.; James, T. G. *J. Org. Chem.* **1995**, *60*, 8294−8304.
(59) Anderson, G. B.; Yang, L. L.-N.; Falvey, D. E. *J. Am. Chem. Soc.* **1993**, *115*, 7254−7262.
(60) Srivastava, S.; Falvey, D. E. *J. Am. Chem. Soc.* **1995**, *117*, 10186−10193.
(61) McIlroy, S.; Moran, R. J.; Falvey, D. E. *J. Phys. Chem. A* **2000**, *104*, 11154−11158.
(62) Srivastava, S.; Kercher, M.; Falvey, D. E. *J. Org. Chem.* **1999**, *64*, 5853−5857.

Scheme 9

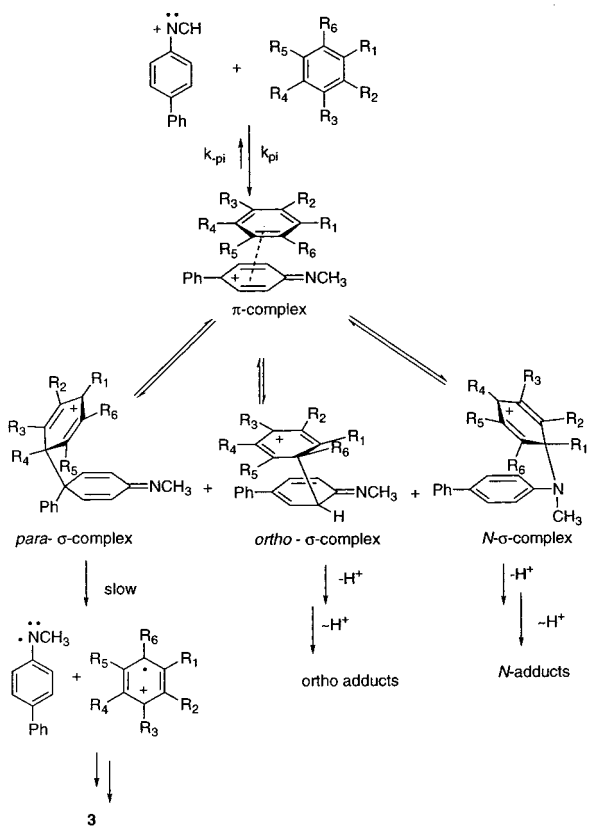

DFT (BPW91/cc-pVDZ) calculations, which were in turn validated through experimental time-resolved infrared characterization of the same species.[21] Moreover, the radical intermediates expected from such a process have not been detected in the LFP experiments. On the basis of this, it seems reasonable to exclude a triplet state mechanism.

Several observations argue against a direct hydride transfer mechanism. First, TEB, which ought to create a more stable secondary carbocation from hydride transfer, reacts more slowly than MES. If the rate-determining step were hydride abstraction, one would expect the opposite result. Second, simple ethers, such as tetrahydrofuran, are expected to be much better hydride transfer agents than the alkoxybenzenes inasmuch as hydride transfer from this species would generate a more substituted, and presumably more stable, oxenium ion. Yet THF reacts more slowly than any (5×10^4 M^{-1} s^{-1}) of the alkoxybenzene derivatives. Likewise, 2-propanol, if it carried out hydride transfer, ought to be more reactive than either THF or any of the primary alcohols. In fact, this secondary alcohol reacts more slowly than any of the primary alcohols (ethanol, *n*-butyl alcohol) and at approximately the same rate constant as *tert*-butyl alcohol, a species which cannot generate a stable oxenium ion.

As a final test for hydride transfer, a kinetic isotope effect experiment was carried out. Specifically, we compared the k_{trap} for 1,4-DMB and for 1,4-DMB-d_6, where the deuteriums were specifically incorporated into the methoxy groups. The measured values were $(8.9 \pm 0.6) \times 10^6$ M^{-1} s^{-1} for the unlabeled trap and $(9.7 \pm 0.5) \times 10^6$ M^{-1} s^{-1} for the labeled trap. It is not clear if the apparent inverse isotope effect is significant given the experimental uncertainty, and if so what the mechanistic consequences of such a result would be. However, it is clear that this result is inconsistent with a significant contribution of hydride transfer to the observed rate constant. It should be stressed that these arguments pertain only to the observed rates of the trapping reactions and not to the overall process. It is clear from the structure of the product that a net hydride transfer must occur. The discussion below will elaborate on this point. These considerations only argue against this occurring in the observed trapping step.

The trends in trapping rate constants and the structures of the products can be accounted for in the π-complexation model illustrated in Scheme 9. In this mechanism, the primary step is the formation of a delocalized π-complex between the arene and the arylnitrenium ion (k_{pi}). The latter intermediate can either dissociate (k_{-pi}) or further collapse to form at least three σ-complexes: one leading to the ortho-adduct, one leading to the N-adduct, and one involving bond formation to the para-position on the nitrenium ion (regiochemical preferences with respect to the arene were not explicitly investigated). (In fact, the substitution patterns on the traps generally permit only one type of adduct). The first two σ-complexes further deprotonate and tautomerize to give the ortho- and N-adducts. Given this mechanism and the assumption that the reaction of the π-complex is slow relative to the preequilibrium, the trapping rate constants measured by LFP, k_{trap}, are related to k_{pi} by eq 8, where k_{rxn} represents the sum of the rate constants for the subsequent steps leading to the products.

$$k_{trap} = \frac{k_{pi}k_{rxn}}{k_{-pi}} \tag{8}$$

A comparison of relative trapping yields from the 1,4-DMB and MES and the LFP-determined rate constants can provide additional insight into the reaction mechanism. The ratio of k_{DMB}/k_{MES} from the LFP experiment is 97, whereas the value from competitive trapping is 183. This suggests that the formation of the π-complex is reversible and that 1,4-DMB undergoes the first irreversible steps toward adducts more rapidly.[63]

The para σ-complex does not give rise to any detectable adducts. This contrasts with results of McClelland and Novak where substantial yields of para-adducts are seen when 4-biphenylylnitrenium ion reacts with water.[35,42,50,64] Perhaps a more relevant example is a study by Novak where the addition of *N*,*N*-dimethylaniline to 4-biphenylylnitrenium ion was examined.[29] In this case, one adduct results from para addition followed by a net 1,2-shift of the phenyl ring providing a meta adduct (Scheme 3).

It appears that several features of the present system prevent formation of these meta-adducts. First, the trapping reactions were carried out in an aprotic solvent with added acid, rather than in buffered aqueous media. The meta product requires a general base to abstract a proton from the meta position in the cyclic intermediate to trigger the shift of the aryl ring. This

(63) Taken alone, the discrepancy in rate ratios might be seen as evidence that the adducts are not derived from the LFP-detected intermediates. However, several observations argue against this. First, the previously published TRIR study (ref 21) leaves little doubt that the LFP intermediate is nitrenium ion **1**. Second, the LFP kinetic studies make clear that nitrenium ion **1** reacts in some manner with the arenes once it is generated. Third, it is unlikely that the adducts are formed from a precursor to nitrenium ion **1**, since addition of arene has no apparent effect on the initial intensity of the nitrenium ion's LFP signal.

(64) McClelland, R. A. *Tetrahedron* **1996**, *52*, 6823−6858.

Scheme 10

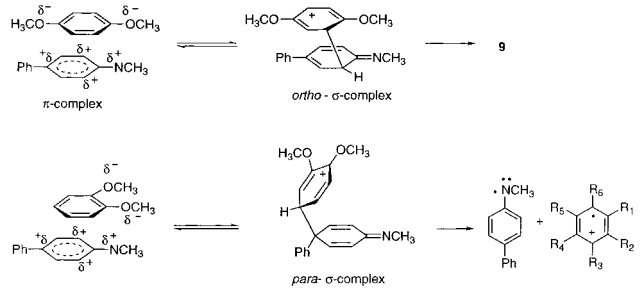

proton abstraction is likely to be much slower in the present system. We suggest that the initial para σ-complex survives for a much longer time period, and then decays through relatively slow homolytic bond scission, which would create an amine radical along with the cation radical of the trap. That such radical intermediates are not detected in the LFP experiments can be attributed to the relatively long lifetime of the σ-complex, which, in turn, generates the radicals in low steady-state concentrations. The observation of some trap dimers and other side products characteristic of the corresponding trap cation radicals is consistent with this. The amine radicals are ultimately transformed into the parent amines through additional reduction steps. Thus, the consequence of para addition is the eventual formation of the reduction product **3**.

It is possible that the N-σ and ortho-σ complexes also undergo an analogous homolytic reaction. This would compete with the tautomerization and deprotonation leading to the stable adducts. The rate of the homolytic dissociation is likely enhanced when there is significant steric compression between the trap and the nitrenium ion. Thus, the highly reactive HMB is seen to give only the parent amine and no adducts. In contrast, MES, which has a lower k_{trap} than HMB, gives significant amounts of the ortho adduct. MES has the electron-donating methyl groups optimally situated to stabilize the ortho σ-complex. This presumably compensates for the destabilizing steric effects, slowing homolysis and allowing for the proton shifts required to generate the stable adducts.

1,2-DMB, whose σ-adducts are stabilized by only one para methoxy group, but destabilized by a meta methoxy group, gives mostly the parent amine with only traces of an adduct detected by GC/MS. Of course, the electronic destabilization argument would seem to predict that the 1,4-DMB should also give low yields of adduct and high yields of parent amine for the same reason that 1,2-DMB does. Interestingly, this is not the case. The 1,4-isomer actually gives predominantly the ortho-adduct. This can be traced to the most likely orientation of the π-complex and the relative rates for formation of the ortho σ-adduct and the para σ-adduct. As depicted in Scheme 10, the 1,4-DMB π-complex places the negatively polarized methoxy groups over the para and nitrenium ion centers on **1**. Steric repulsion disfavors collapse to the para σ-complex and favors formation of the ortho σ-complex. In contrast, 1,2-DMB forms a π-complex which has one methoxy over the nitrenium ion center and one over the ortho carbon. This orientation disfavors formation of the ortho σ-adduct and shows far less steric repulsion for formation of the para σ-adduct. It is assumed that the latter eventually suffers homolysis and eventually leads to the parent amine.

Formation of reduction product requires the addition of a second electron. The observation of the insertion product **15**, and hydroxymethylpentamethylbenzene **16**, would indicate that the additional electron (or H atom) is derived from a subsequent electron or H atom transfer from the arene radical cation. Because the initial radical pair forms from a singlet σ-adduct, the resulting radical−radical ion pair must be initially formed in the singlet state. This would make the secondary H atom transfer or electron transfer fast relative to cage escape and would also reduce the yield of observable radicals in the LFP experiment. This mechanism is diagrammed in Scheme 11 for the case of HMB. H atom transfer from the cation radical of HMB to the amine radical **14** gives **3** and the HMB cation **18**. This pair can undergo a further coupling to produce adduct **15**, or the cation can react with adventitious water to yield **15**.

Scheme 11. Formation of Reduction Product **3** from HMB

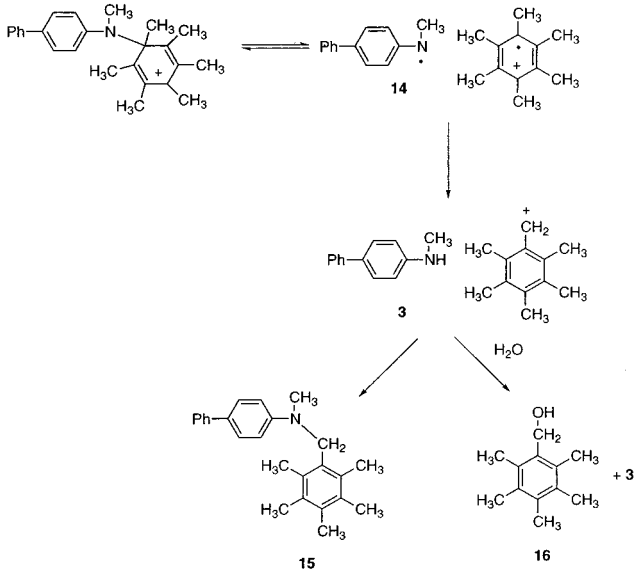

Scheme 12

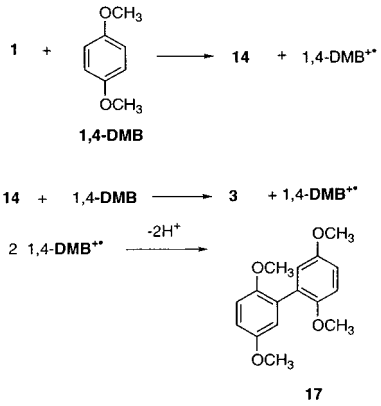

An alternative route to the parent amine **3** is illustrated by the formation of the 1,4-DMB dimer **17**. Previous studies have shown that this product forms from the coupling of two 1,4-DMB cation radicals.[65,66] In this case, it appears that dissociation of the 1,4-DMB σ-adduct produces 1,4-DMB cation radicals. Under these circumstances, **3** is formed from oxidation of a second 1,4-DMB molecule by radical **14** (Scheme 12).

The ratio of N-addition to ortho-addition, on the other hand, does correlate with the reactivity of the arene. In fact, the only

(65) Nishinaga, A.; Hayashi, H.; Matsuura, T. *Bull. Chem. Soc. Jpn.* **1974**, *47*, 1813−1814.
(66) O'Neill, P.; Steenken, S.; Schulte-Frohlinde, D. *J. Phys. Chem.* **1975**, *79*, 2773−2779.

cases where N-adducts are observed are with the most reactive traps, TMB and 1,3-DMB, and even then, these are minor products relative to the ortho-adduct and parent amine. This result conforms to a trend that was first observed in the trapping of Ph_2N^+ by electron-rich alkenes.[30] With the least reactive alkenes, the products resulted from addition of the alkene to the ortho and para ring on the arylnitrenium ion. Only with the most electron-rich alkenes were small amounts of N-adduct seen. Thus, it appears that even for π-nucleophiles there is a kinetic preference for addition to the ring carbons of arylnitrenium ions.

This contrasts with arylcarbenium ions which add nucleophiles to the exocyclic carbon atom almost exclusively. Novak et al.[50] have attributed this tendency to differences in the aromaticity of the carbenium ions as compared with that of the corresponding arylnitrenium ions. The arylcarbenium ion's phenyl ring possesses more aromatic character, which would presumably be lost in the event of ring addition by the nucleophile. In contrast, the arylnitrenium ion is more accurately described as an iminecyclohexadienyl cation.[16−18,20,21,67] Thus, nucleophilic addition to the aromatic ring in this latter case does not remove aromatic character. The regiochemical results described herein further emphasize the unusual behavior of guanosine as a nucleophile. This species appears to react exclusively at the nitrenium ion's nitrogen. The reasons for this remain uncertain. However, it is possible that this reaction may occur via a mechanism that differs from the simple arenes examined here.

Experimental Section

LFP Experiments. Laser flash photolysis (LFP) data were collected using either an XeCl excimer laser (308 nm) or the third harmonic (355 nm) of a pulsed Continuum Surelite II-10 Nd:YAG laser (<5 mJ/pulse, 4−6 ns). During a given experiment, the pulse energy varied by <5%. The transient behavior was monitored using a probe beam from an Oriel CW 400 W Xe arc lamp passed through the sample cuvette perpendicular to the excitation beam. Transient waveforms were recorded with a LeCroy 9420 digital oscilloscope which digitizes at a rate of one point/10 ns with a bandwidth of 350 MHz. Programs developed in our laboratory, using MATLAB 4.2 and LabView 5.0 software, were used in processing the LFP data.

Samples for pulsed irradiation were prepared such that the absorbance of substrate **2** was approximately 2.0 at 355 nm. LFP transient spectra were based on pulsed irradiation of a single 3.0 mL sample of pyridinium salt substrate when photolyzing at 355 nm with concentrated solutions. Low sample depletion was confirmed by steady-state UV spectrum measurement of the sample following the LFP data collection. These samples were purged throughout the experiment with N_2. Frequent displacement of sample solution with fresh stock solution during data collection assured that transient spectra were not affected by excessive depletion of substrate or accumulation of photoproducts.

Stable Products from Arene Trapping. These experiments involved preparation of stock solutions containing **2**, arene, or other trap, and small amounts of concentrated $HClO_4$ (70%) in CH_3CN solvent. Solutions were purged with N_2, and photolyzed only above 320 nm using an appropriate cutoff filter (320 nm) and an Oriel CW 400 W Xe arc lamp. Photolyzed solutions were concentrated under reduced pressure and dissolved in CD_3CN with 1% TMS for calibration of chemical shift. The percentage conversion of substrate **2** following photolysis was calculated using appropriate peaks in the ^1H NMR spectrum of crude, concentrated photolyzate. This was accomplished using methyl group signals of protonated 2,4,6-collidine (6H at 2.60 ppm, 3H at 2.53 ppm) and the 2,4,6-trimethylpyridinium moiety of remaining **2** (6H at 2.48 ppm, 3H at 2.58 ppm). Integrations in ^1H NMR spectra also provided estimates of the yield of amine **3** and, in some cases, various adducts. Absolute yields were calculated on the basis of the integration of the 3.10 ppm signal of the N-methyl group of $3H^+$ or integrations of other peaks specified. In preparative photolyses, stated yields of isolated photoproducts are based on mole amounts of converted substrate **2** which are estimated by ^1H NMR.

GC/MS analysis was frequently employed following workup of concentrated CD_3CN solutions from crude photolysis mixtures. In preparative photolyses, standard workup conditions involved the addition of roughly equal volumes of CH_2Cl_2 and aqueous $NaHCO_3$ to concentrated crude photolyzate. Small samples for GC/MS analysis were taken from organic layers following extraction with CH_2Cl_2. Standard workup procedure for small scale photolyses involved dilution of CD_3CN solution to 5.0 mL with CH_2Cl_2 and the addition of 5.0 mL of aqueous $NaHCO_3$. The two-phase system was shaken, and the CH_2Cl_2 layer was sampled for GC/MS.

Preparative Photolysis of 2 with TMB. Two separate and nearly identical stock solutions were prepared and photolyzed over the course of several days. The first 50.0 mL stock solution contained 50.1 mg of **1b**, 360 mg of TMB, and 40 μL of $HClO_4$ (70%) for respective concentrations of 2.57, 42.9, and 9.3 mM. The second 50.0 mL stock solution contained 51.1 mg of **1b**, 361 mg of TMB, and 40 μL of $HClO_4$ (70%) for respective concentrations of 2.62, 43.0, and 9.3 mM. The slight differences in the two stock solutions were considered negligible in affecting the resulting product distributions. Both solutions were divided into 5.0 mL portions, and each portion was purged with N_2 throughout 40 min of photolysis. Photolyzed samples from both stock solutions were combined and stored in a dark freezer until all 20 5.0 mL portions were photolyzed. The cumulative photolyzate was sampled (5.0 mL) and concentrated under reduced pressure for ^1H NMR analysis. Percentage conversion was calculated to be 88.5% using the general method described. The recombined solution was concentrated under reduced pressure, added to aqueous $NaHCO_3$, and extracted three times with CH_2Cl_2. CH_2Cl_2 extracts were combined and dried over $MgSO_4$ before concentrating for column chromatography. Eluting with 15% EtOAc/85% hexanes, fractions were concentrated individually and analyzed by TLC. Combining appropriate fractions (some mixed fractions not included) and concentrating under reduced pressure, the following photoproducts were obtained: 8.9 mg of amine **3**, with an estimated additional 8 mg in fractions contaminated with TMB (determined by ^1H NMR) for total estimated yield of 17 mg of **3b** (0.093 mmol, 43%, characterized by ^1H NMR for comparison to the spectrum of the authentic compound); 20.9 mg of ortho ring adduct **5** (0.060 mmol, 27%). ^1H NMR (400 MHz, $CDCl_3$): δ 7.57 (dd, J = 8.3, 1.1 Hz, 2H), 7.53 (dd, J = 8.4, 2.3 Hz, 1H), 7.36 (t, J = 7.7 Hz, 2H), 7.29 (d, J = 2.3 Hz, 1H), 7.23 (t, J = 7.7 Hz, 1H), 6.78 (d, J = 8.4 Hz, 1H), 6.26 (s, 2H), 3.88 (s, 3H), 3.72 (s, 6H), 3.70 (br s, 1H), 2.84 (s, 3H). ^{13}C NMR (100 MHz, $CDCl_3$): δ 161.1, 159.1, 147.2, 141.6, 130.5, 129.2, 128.4, 127.0, 126.3, 125.6, 120.2, 110.0, 108.3, 91.1, 56.0, 55.4, 31.1. MS (FAB) m/z (relative intensity): 351 (24), 350 ([M + H]$^+$, 100), 349 (43), 335 (12), 318 (11). HRMS (FAB): calcd for $C_{22}H_{24}NO_3$, 350.17563; found, 350.17689. 8.0 mg of N-adduct **6** (0.023 mmol, 11%) ^1H NMR (400 MHz, $CDCl_3$): δ 7.53 (dd, J = 8.0, 1.1 Hz, 2H), 7.41 (d, J = 8.7 Hz, 2H), 7.36 (t, J = 7.5 Hz, 2H), 7.21 (t, J = 7.5 Hz, 1H), 6.57 (d, J = 8.7 Hz, 2H), 6.21 (s, 2H), 3.86 (s, 3H), 3.74 (s, 6H), 3.19 (s, 3H). ^{13}C NMR (100 MHz, $CDCl_3$): δ 158.5, 158.4, 148.5, 141.7, 132.3, 128.6, 128.5, 127.4, 126.2, 125.6, 111.9, 91.4, 56.0, 55.4, 38.6. MS (EI) m/z (relative intensity): 350 (24), 349 (100), 334 (17), 167 (27), 152 (15). HRMS (FAB): calcd for $C_{22}H_{24}NO_3$, 350.17563; found, 350.17509.

Preparative Photolysis of 2 with 1,3-DMB. A 50 mL stock solution was prepared which contained 49.6 mg of **1b**, 0.598 g of 1,3-DMB, and 40 μL of $HClO_4$ (70%) in MeCN solvent for respective concentrations of 2.54, 86.6, and 9.3 mM. The stock solution was divided into

(67) Cramer, C. J.; Falvey, D. E. *Tetrahedron Lett.* **1997**, *38*, 1515−1518.

10 5.0 mL portions, and nine of these were purged with N_2 and photolyzed (>320 nm) for 40 min each. Recombining portions, the photolyzate was sampled (5.0 mL aliquot) and concentrated under reduced pressure to obtain a crude ^{1}H NMR spectrum. On the basis of the general procedure, substrate conversion was calculated to be 90%. Recombined crude photolyzate was added to aqueous $NaHCO_3$ and extracted three times with CH_2Cl_2. CH_2Cl_2 extracts were combined, dried over $MgSO_4$, and concentrated under reduced pressure for column chromatography. Eluting with 12% EtOAc/88% hexanes, fractions were collected and analyzed by TLC. Excess 1,3-DMB was the first eluted compound followed by the N-adduct **13**, amine **3b**, and the ortho ring adduct **12**. By combining appropriate fractions and removing solvent under reduced pressure and moderate temperatures (<45 °C), these major photoproducts were isolated: 9.4 mg of **3** (0.051 mmol, 49%, characterized by ^{1}H NMR which matched spectrum of authentic compound); 7.0 mg of **7** (0.022 mmol, 21%). ^{1}H NMR (400 MHz, $CDCl_3$): δ 7.55 (dd, J = 8.2, 1.1 Hz, 2H), 7.52 (dd, J = 8.4, 2.3 Hz, 1H), 7.36 (t, J = 7.7 Hz, 2H), 7.33 (d, J = 2.3 Hz, 1H), 7.22 (t, J = 7.7 Hz, 1H), 7.18 (d, J = 7.2 Hz, 1H), 6.83 (br d, J = 8.4, 1H), 6.59−6.56 (m, 2H), 4.32 (br s, 1H), 3.85 (s, 3H), 3.76 (s, 3H), 2.83 (s, 3H). MS (FAB) *m*/*z* (relative intensity): 320 ([M + H]$^+$, 27), 149 (25). HRMS (FAB): calcd for $C_{21}H_{22}NO_2$, 320.16504; found, 320.16407. 7.4 mg of **8** (0.023 mmol, 22%) ^{1}H NMR (400 MHz, $CDCl_3$): δ 7.53 (dd, J = 8.1, 1.0 Hz, 2H), 7.41 (d, J = 8.7 Hz, 2H), 7.37 (t, J = 7.5, 2H), 7.23 (t, J = 7.5 Hz, 1H), 7.12 (d, J = 8.5 Hz, 1H), 6.66 (d, J = 8.7, 2H), 6.58 (d, J = 2.7 Hz, 1H), 6.51 (dd, J = 8.5, 2.7 Hz, 1H), 3.84 (s, 3H), 3.76 (s, 3H), 3.22 (s, 3H). ^{13}C NMR (100 MHz, $CDCl_3$): δ 159.1, 157.1, 149.2, 141.3, 130.0, 129.5, 129.3, 128.6, 127.4, 126.2, 125.8, 112.9, 104.6, 100.2, 55.7, 55.5, 39.3. MS (EI) *m*/*z* (relative intensity): 320 ([M + H]$^+$, 26), 319 (100), 304 (18), 167 (22). HRMS (EI): calcd for $C_{21}H_{21}NO_2$, 319.15723; found, 319.15857.

Preparative Photolysis of 2 with 1,4-DMB. A solution was prepared which contained 35.0 mg of **2**, 69.2 mg of 1,4-DMB, and 20 μL of $HClO_4$ (70%) in 20 mL of MeCN for respective concentrations 4.48, 25.1, and 11.6 mM. This solution was divided into two equal portions, and each was purged with nitrogen and photolyzed for 25 min using a 320 nm cutoff filter. Recombined photolyzates were sampled for crude ^{1}H NMR analysis. Approximately 69% (0.062 mmol) of **2** was photodecomposed. The CD_3CN solution of product mixture was recombined with photolyzate and concentrated under reduced pressure. The residue was taken up in CH_2Cl_2 and combined with aqueous $NaHCO_3$ solution, extracting twice with CH_2Cl_2. The organic layer was dried over $MgSO_4$ and concentrated for column chromatography. Eluting with 15% EtOAc/85% hexanes, the following compounds were obtained: 3.1 mg of **3** (0.017 mmol, 27%, characterized by ^{1}H NMR for comparison to the spectrum of the authentic compound); and 13.3 mg (0.0417 mmol, 67%) of **9** (with traces of DMB dimer **17** < 5%). ^{1}H NMR (400 MHz, CD_3CN): δ 7.57 (dd, J = 8.2, 1.1 Hz, 2H), 7.51 (dd, J = 8.4, 2.3 Hz, 1H), 7.37 (t, J = 7.7 Hz, 2H), 7.27 (d, J = 2.3 Hz, 1H), 7.21 (tt, J = 7.3, 1.0 Hz, 1H), 7.01 (d, J = 9.0 Hz, 1H), 6.93 (dd, J = 9.0, 3.1 Hz, 1H), 6.79 (d, J = 3.1 Hz, 1H), 6.65 (d, J = 8.4 Hz, 1H), 4.05 (br s, 1H), 3.75 (s, 3H), 3.70 (s, 3H), 2.76 (s, 3H). ^{13}C NMR (100 MHz, $CDCl_3$): δ 154.0, 151.1, 146.3, 141.2, 129.5, 129.3, 128.9, 128.5, 127.3, 126.3, 125.9, 124.8, 117.3, 114.1, 112.9, 110.3, 56.6, 55.7, 30.9. MS (EI) *m*/*z* (relative intensity): 319.1 (M$^+$, 100), 273.1 (37). HRMS (EI): calcd for $C_{21}H_{21}NO_2$ (M$^+$), 319.15723; found, 319.15700.

Preparative Photolysis of 2 with MES. A stock solution was prepared which contained 40.0 mg of **2**, 0.85 g of **MES**, and 40 μL of $HClO_4$ (70%) in 50 mL of MeCN, for respective concentrations of 2.05 mM, 0.142 M, and 9.3 mM. The stock solution was divided into 10 5.0 mL portions, and each was purged with N_2 and photolyzed (>320 nm) for 1 h. The percentage of photodecomposition of **2** as measured by ^{1}H NMR spectra of concentrated crude photolyzate was 96 ± 3% in all cases. Combined samples were added to aqueous $NaHCO_3$ and extracted three times with CH_2Cl_2. CH_2Cl_2 extracts were combined, dried over $MgSO_4$, and concentrated under reduced pressure for column chromatography. Eluting with 20% EtOAc/80% hexanes, fractions were collected and analyzed by TLC. The following photoproducts were isolated: 7.2 mg of parent amine **3** (0.039 mmol, 44%, characterized by ^{1}H NMR and matched spectrum of authentic standard); and 13.9 mg (0.0461 mmol, 52%) of adduct **12**. ^{1}H NMR (400 MHz, $CDCl_3$): δ 7.57−7.53 (m, 3H), 7.36 (t, J = 7.6 Hz, 2H), 7.20 (t, J = 7.6 Hz, 1H), 6.98 (s, 2H), 6.75 (d, J = 8.4 Hz, 1H), 2.80 (s, 3H), 2.34 (s, 3H), 2.02 (s, 6H). ^{13}C NMR (100 MHz, $CDCl_3$): δ 145.8, 141.3, 137.4, 137.2, 134.6, 129.5, 128.6, 128.5, 128.0, 126.7, 126.2, 126.1, 125.9, 109.8, 30.7, 21.1, 20.2. MS (FAB) *m*/*z* (relative intensity): 303 (25), 302 ([M + H]$^+$, 100), 301 (74), 300 (21), 287 (11), 285 (12), 271 (10), 255 (10). HRMS (FAB): calcd for $C_{22}H_{24}N$, 302.19089; found, 302.18948.

Competitive Photolysis of 1 with 1,4-DMB and MES. A solution was prepared which contained 30.3 mg of **2** and 30 μL of $HCLO_4$ (70%) in 30 mL of MeCN for respective concentrations of 2.56 and 11.6 mM. To a 10 mL aliquot of this solution was added 200 μL of MES (144 mM) and 36.6 mg of 1,4-DMB (26.5 mM). The solution was purged with N_2 and photolyzed for 30 min using a Nd:YAG laser emitting at 355 nm (100 mJ/pulse, 10 Hz, 4−6 ns pulse length) with continuous stirring. The photolyzate was washed with 10 mL of aqueous $NaHCO_3$ and extracted three times with CH_2Cl_2. The organic layer was dried over $MgSO_4$, and the solvent was then removed. The residue was taken up in 2 mL of MeCN for GC analysis. The final concentrations were determined to be 4.79 mM (37.4% yield) **3**, 4.91 mM (38.3% yield) **9**, and 0.106 mM (0.826% yield) **12**.

Acknowledgment. This work was supported by the Chemistry Division of the National Science Foundation.

Supporting Information Available: Relationship of trapping rate constants (k_{trap}) for the arenes to the equilibrium constant for addition of HF to the same arenes (PDF). This material is available free of charge via the Internet at http://pubs.acs.org.

JA011049N